International Journal of Wireless and Mobile Computing

ISSN online: 1741-1092 - ISSN print: 1741-1084
https://www.inderscience.com/ijwmc

Fracture constitutive study of spring-beam model applied to slurry anchor connection

Wenjun Zhou, Shipian Shao, Hongxin Nie, Li Ma

DOI: 10.1504/IJWMC.2024.10061994

Article History:

Received:	29 October 2023
Last revised:	08 December 2023
Accepted:	19 December 2023
Published online:	04 March 2024

Fracture constitutive study of spring-beam model applied to slurry anchor connection

Wenjun Zhou*

School of Civil Engineering,
Jilin University of Architecture and Technology,
Changchun, Jilin, China
Email: 1730219815@qq.com
*Corresponding author

Shipian Shao

School of Management,
Shenyang Jianzhu University,
Shenyang, Liaoning, China
Email: shaosp0806@163.com

Hongxin Nie

School of Civil Engineering,
Jilin University of Architecture and Technology,
Changchun, Jilin, China
Email: 312485538@qq.com

Li Ma

China State Construction Railway Investment &
Engineering Group Co., Ltd.,
Changchun, Jilin, China
Email: 981622653@qq.com

Abstract: In order to prove the feasibility of selecting the beam element attributes of the spring-beam model by parameter prediction algorithm, this study proposes a beam elements fracture constitutive model that simulates the fracture of mortar and concrete at the slurry anchor connection. By adjusting the elastic modulus, plastic strain, fracture modulus and section properties of beam elements, the results of literature tests are compared with the finite element calculation and the effects of key parameters in the beam elements fracture constitutive calculation model are analysed. The results show that the calculated slip deformation of the slurry anchor connection is controlled by the plastic strain and fracture modulus of beam elements. The mortar entry to the plasticity calculation stage is controlled by section properties of beam elements. The overall deviation of calculation from experimental results is controlled by the elasticity modulus of beam elements, and the parameter optimal solution has uniqueness.

Keywords: spring-beam; fracture of beam element; slurry anchor; mortar; concrete.

Reference to this paper should be made as follows: Zhou, W., Shao, S., Nie, H. and Ma, L. (2024) 'Fracture constitutive study of spring-beam model applied to slurry anchor connection', *Int. J. Wireless and Mobile Computing*, Vol. 26, No. 2, pp.107–114.

Biographical notes: Wenjun Zhou is a Lecturer in the Department of Civil Engineering at Jilin University of Architecture and Technology. He has a Master's degree in Structural Engineering. His research focuses on computational mechanics and structural safety.

Shipian Shao is the Graduate student of School of Management at Shenyang Jianzhu University of China. She Graduated from Shenyang Jianzhu University in 2021 with a Bachelor's degree in Management. She is mainly engaged in the research of low-carbon technology innovation and sustainable development.

Hongxin Nie is a Lecturer in the Department of Civil Engineering at Jilin University of Architecture and Technology. She has a Master's degree in Structural Engineering. Her research focuses on building earthquake resistance and structural safety.

Li Ma is an Engineer at China state Construction Railway Investment & Engineering Group Co., Ltd. He is a Bachelor's degree in Structural Engineering. His focuses on building earthquake resistance and structural safety.

1 Introduction

Precast concrete unit reinforcement connection form mainly has sleeve grouting connection and constrained slurry anchor connection. Sleeve grouting connection technology is suitable for frame structure of larger diameter reinforcement connection. It is widely used at home and abroad, but asks for high requirement for equipment and technical level of construction personnel, also has high-economic costs. Slurry anchor connection construction process is simple, low-economic cost, widely used in shear wall structure system, but the corresponding technology application standard is not mature. Therefore, the study of mechanical properties of slurry anchor connection has far-reaching significance.

Domestic and foreign scholars have spent a lot of efforts in the experimental research of constrained slurry anchor connection. Thirty-three restrained slurry anchor connection joint specimens were designed in 2018, and uni-directional tensile, high-stress repeated tensile and compression and large deformation repeated tensile and compression tests were carried out, which proved that the slurry anchor connection form has sufficient strength, good connection force transfer effect, and is a reliable precast concrete unit reinforcement connection form (Xie et al., 2018). Wu et al. (2020) conducted weak repeated loading tests on a slurry anchor connection assembled shear wall space structure model and concluded that the slurry anchor connection has two weak surfaces at the edge of the lap zone. It is recommended to pay attention to the reasonable design of connecting beams in prefabricated shear walls (Wu et al., 2020). Guo et al. (2022) designed 18 groups of connections to complete the pullout test and concluded that the anchorage length should not be less than 10 d in practical engineering to ensure that the steel bars make full use of mechanical properties in normal operation. Wu et al. (2009) used steel bar-metal bellows slurry anchor connection to achieve the assembling of steel beams and prefabricated concrete columns, and researched the seismic performance of the composite frames using this connection. Hosseini et al. (2015, 2016) researched that spiral hoops and hoop spacing have an impact on the anchorage performance of steel bar-metal bellows slurry anchor connection, and concluded that the slip was smaller when the hoop spacing was 25 mm.

The large amount of experimental research has laid a research foundation for the finite element method being applied to the research and development projects of slurry anchor connection structure. Shi et al. (2021) used the finite element method to analyse mechanical behaviour under axial tension and compared with the experimental results to verify the accuracy of the numerical simulation study. Zhou et al. (2021a) proposed the spring-rod model and the spring-beam model using finite element calculation of slurry-anchor connection , in which the concrete damage state, hysteresis curve and equivalent stiffness of slurry-anchor-connected prefabricate shear wall calculated by the spring-beam model are closer to the experimental results and conform to modelling standards, and using the spring-beam model to simulate the force of slurry-anchor connection, its results can be consistent with the actual conclusion (Zhou et al., 2021b). Nie et al. (2022) adopt 'Spring-beam-block' element model to research the finite element calculation problem of reinforcing sleeve grouting connection, drawing the ideal control range of spring elements stiffness and beam elements.

This dissertation adopts finite element calculation and test results comparison methods, not only improve the 'spring-beam' model, but also to put forward the slurry-anchor connection beam element fracture constitutive model, and analyses the impact of key parameters of the constitutive model on the deformation and fracture of the grouting mortar, arguing for predictability of key parameter resolutions, laying a foundation for the subsequent research of spring elements stiffness and beam elements constitutive prediction model.

2 Spring-beam model description

2.1 Slurry anchor connection

Grout-anchor connection is the precast concrete unit surface outstretched a certain length of discontinuous steel bars inserting into the reserved aperture of the connected precast concrete unit corresponding position, steel bars and the aperture wall filling with non-shrinkage, high-strength grout, grouting and hardening after the completion of the reinforcement lap. Figure 1 illustrates the structure of slurry anchor connection.

2.2 Spring-beam model

Several test results show that the damage patterns of the specimens are mainly four kinds: bar pull-out, split pull-out, bar pull-off and split pull-off. The spring-beam model divides the damage of slurry-anchor connection node into two stages, the first stage is bond damage, the time before (including the time of) steel bars break with mortar and concrete and the second stage is slip damage, the time after the mortar breaks with steel bars and concrete. The first stage relies on the beam elements simulation, and the second stage relies on the spring elements simulation, so as to accurately reflect the strength failure of the mortar-anchor connection at the time of its occurrence and the slip detachment afterwards. This article focuses on the first stage. Figure 2 shows the spring-beam model.

Figure 1 The structure of slurry anchor connection

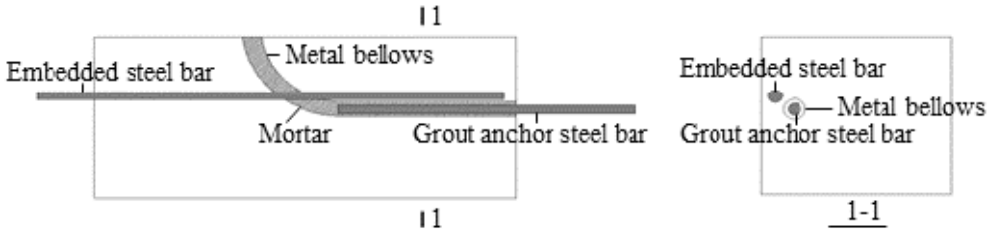

Figure 2 The spring-beam model

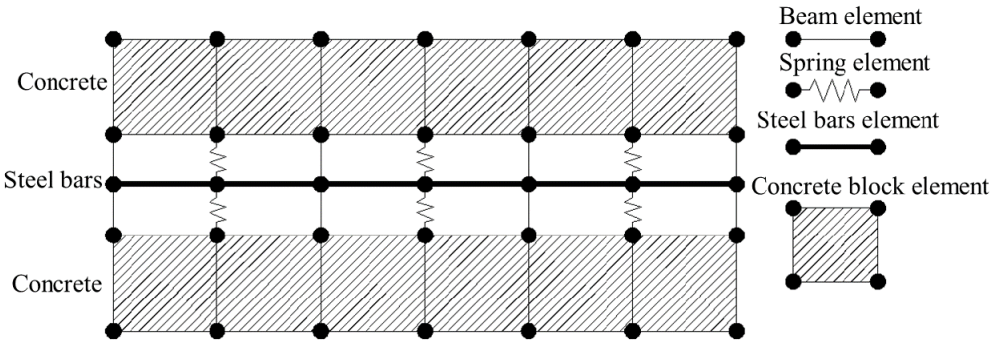

3 Beam element fracture calculation model

3.1 The proposal of fracture constitutive model

The bond strength decreases with the increase of steel bars anchorage length and diameter; with the increase of bellows diameter, the bond strength varies non-linearly with the steel bars diameter (Zhao et al., 2023). Therefore, the application of the spring-beam model to simulate the slurry-anchor connection node, to ensure that the simulation results coincide with the actual force conditions of specimens, to accurately predict the stiffness of spring elements according to the anchorage length and diameter of the steel bars as well as the diameter of the bellows, and to determine the structure of beam elements. This is a prerequisite for the application of the spring-beam model in engineering practice.

Before the bond failure of mortar, steel bars and concrete occur, the mortar at the location of bond damage undergoes elastic deformation, plastic deformation and fracture damage process. The beam element fracture constitutive model is proposed to simulate mortar behaviours before bond damage, which is a four-segment curve: 0—ε_e, the beam element stress grows linearly (mortar elasticity); ε_e—ε_p the beam element stress maintains a constant value and the deformation increases (mortar spasticity); ε_e—ε_b, the beam element stress decreases abruptly (mortar fracture); ε_b+, the beam element stress stays at a very small constant value (mortar adhesion) and deformation increase.

Figure 3 The beam element fracture constitutive calculation model

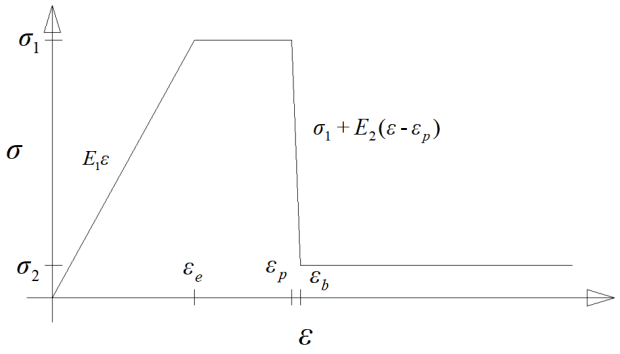

Here, 0—ε_e is the elastic phase of the beam element; ε_e—ε_p is the beam element plastic phase; ε_e—ε_b is the beam element fracture stage; σ_1 is beam element strength, set as the standard value of compressive strength of tar; is weak bond maintained by the beam element at bond breakage; E_1 is eltic module of beam element; E_2 is beam element modulus of rupture.

3.2 The analysis of beam element fracture constitutive calculation model

3.2.1 Specimen materials calculation

Metal bellows mortar anchor steel bar connectors are anchored in metal bellows embedded in concrete filled square

steel column by mortar, and these columns contain 12 connectors. The diameter of steel bar d is set as 18 mm and 25 mm, and the strength grade of steel bar is HRB400. Values of 36 mm and 50 mm are chosen as the aperture diameter of metal bellows respectively, and the anchoring length of steel bar l_a is set as 4d, 7d and 10d, respectively, and d is the diameter of connecting steel bar. The spacing between the axis of the steel bars and the outer wall of the steel pipe c was set as 55 mm. The square steel pipe has the section size of 400 mm × 400 mm × 6 mm, and the steel pipe adopts Q345 grade. The concrete is made of C40, and the strength of grout HBG-A is 62.3 MPa. The specimen parameter table is shown in Table 2 (He, 2020), and the specimen geometry picture is shown in Figures 4 and 5. The elastic-plasticity model is used for the steel bar and the metal bellows and material parameters are shown in Table 1. The concrete adopts plasticity damage model and the C40 concrete adopts the 10-specification concrete material principal model, and other parameters are shown in Table 2.

Table 1 Model parameters

Specimen number	E_1 *(MPa)*	E_2 *(MPa)*	$\varepsilon_p - \varepsilon_e$	*(mm)*	K_{spring} *(N/mm)*
c55-185004	55,000	–61300	0.01	5	150
c55-185007					
c55-185010	90,000				
c55-255004	36,500			16	
c55-255007	26,500			5	
c55-255010	96,500			20	
	26,500				
	36,500				
c55-183607	55,000			8	
	76,500				
	96,500				
	96,500			10	

Table 2 Beam element selection parameters

Specimen number	E_1 *(MPa)*	E_2 *(MPa)*	$\varepsilon_p - \varepsilon_e$	*(mm)*	K_{spring} *(N/mm)*
c55-183607-R8-E36500	36500		0.01	8	150
c55-183607-R9-E36500				9	
c55-183607-R10-E36500				10	

3.2.2 Calculate specimen loading

The test loading device adopts a hydraulic piercing jack with a range of 600 kN, and the piercing anchorage of steel bars adopts a trilobal clip anchorage. The loading rate was 10-15 kN/min until the external load reached 75% of the predicted ultimate load of the connection, after which the loading rate was reduced to 5 kN/min until the damage of the specimen occurred or the jack reached the end of its ultimate stroke to end the loading. The test setup diagram is shown in Figure 2 (He, 2020). The loading method and loading curves in the simulations are kept consistent with the tests.

3.2.3 The assessment and validation of fracture constitutive model

The model parameter E_1.

Adjust parameters E_1, E_2, $\varepsilon_p - \varepsilon_e$ in the mortar fracture calculation model, and take the ultimate strength and deformation in the nodal force-deformation curve of test results as the main optimisation indexes, so as to get the simulation and test force-deformation curves, and the final selection of parameters of the beam element is shown in Table 1.

E_1 can affect the development process of the elastic pose of the nodal force-deformation curve. The same number test specimens, when the elastic modulus E_1 is adjusted from small to large, the finite element simulated force-displacement curve will gradually approach the tested one until the two are close enough to obtain a reasonable E_1 value. In Figure 4, the elasticity modulus of c55-183607 specimen increased from 26,500 to 96,500 MPa.

Figure 4 Force-displacement curves of specimens with different beam element modulus of elasticity c55-183607

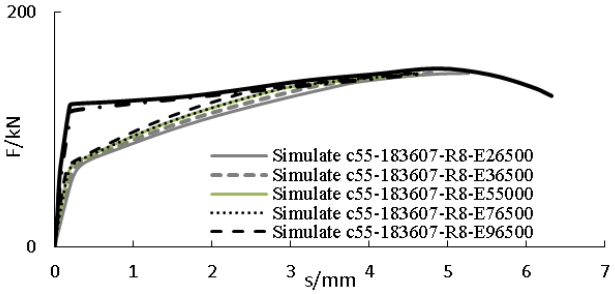

Define S as the sum of the areas enclosed by the test and simulation curves, the size of S representing the degree of deviation of the simulation results away from the test results.

$$S = \int \left| F_T(s) - F_S(s) \right| ds \tag{1}$$

where $F_T(s)$ is the force-displacement curve obtained from the test; $F_S(s)$ is the force-displacement curve obtained from the finite element simulation.

For different numbered test specimens, change steel bars anchorage length of a particular specimen, such as Figures 5(a), 5(b) and 5(c), specimen from c55-185004 to c55-185010, and the reinforcing steel bar anchorage length from 4 to 10d:

$$E_{1a} > E_{1c55-185004} = E_{1c55-185007} > E_{1c55-185010} \tag{2}$$

$$-S_{c55-185004} \approx -S_{c55-185007} < -S_{c55-185010} < \tag{3}$$

Specimen from c55-255004 to c55-255010, such as Figures 5(d), 5(e) and 5(f), and the reinforcing steel bar anchorage length varied from 4 to 10d:

$$E_{1c55-255010} > E_{1a} > E_{1c55-255004} > E_{1c55-255007} \tag{4}$$

$$S_{c55-255010} < 0 < -S_{c55-255004} < -S_{c55-255007} \tag{5}$$

Figure 5 Diagram of deviation degree between test curve and simulation curve

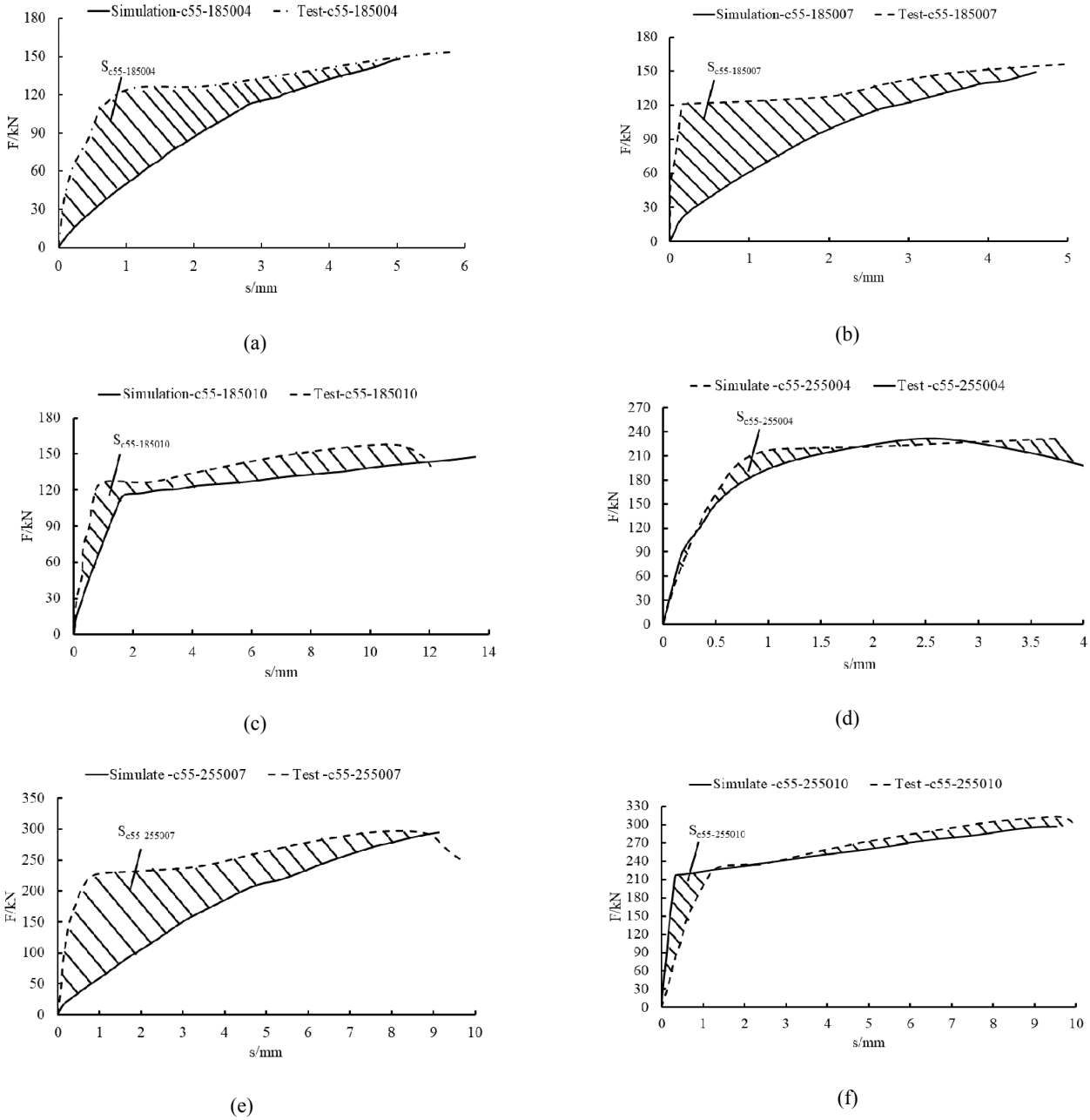

Observing equations (2), (3), (4) and (5), it is found that even if the anchorage length is changing, E_1 can still reflect the degree of proximity between the finite element simulated force-displacement curve and the curve obtained from the test. In theory, there exists an ideal elastic modulus E_{1a} making $S = 0$, that is, the finite element simulated force-displacement curve coincides with the one obtained from the test. As shown in the figure, the simulated curve is extremely close to the test curve when E_{1a} =96,500 MPa and R=10 mm. Meanwhile, other statistics show that $E_1 = E_{\mathrm{HPG-A}}$ (elasticity modulus of mortar material) and $E_1 = E_{1a}$ cannot cause great fluctuation in the finite element simulation force-displacement curve.

The model parameter ε_p , E_2

The mortar fracture is caused by the exceeded strain energy of the beam element, that is the accumulated strain energy in the element exceeds the area S_{E} which enclosed by the calculated mortar fracture constitutive curve and ε-axis. The strain energy S_{E} is the same for the grout-anchor joints with the same mortar material (same beam element σ_{m}) and the same aperture (same beam element l_{beam}). Because the fluctuation range of E_1 is not large, the prediction of ε_{p} must have a range to follow and there exist such an optimal elastic modulus $\varepsilon_{\mathrm{p}} = \varepsilon_{\mathrm{pa}}$ in theory.

The model parameter R_{beam}

As shown in Figure 6, c55-1836007 specimen set $E_1 = 36,500$ MPa , and set R_{beam} from 8 to 10 mm, the moment when the mortar of the specimen c55-1836007 enters into the plastic phase in the simulation is gradually postponed till $R_{beam} = 10$ mm, the mortar is in the elastic phase in the whole loading phase of the s and the closest results to the specimen c55-1836007 are obtained. In summary, the beam element radius R_{beam} is the parameter to control the simulated mortar into the plastic phase. Since the mortar entering the plastic phase is unique for different specimens, R_{beam} is unique. Other statistics show that if the mortar is in the elastic phase throughout the loading stage, R_{beam} can be taken as the minimum value of R_{beam} that makes the mortar in the elastic phase during the loading stage.

Figure 6 Force-displacement curves of 'test c55-1836007' specimen and 'simulate c55-1836007' specimen

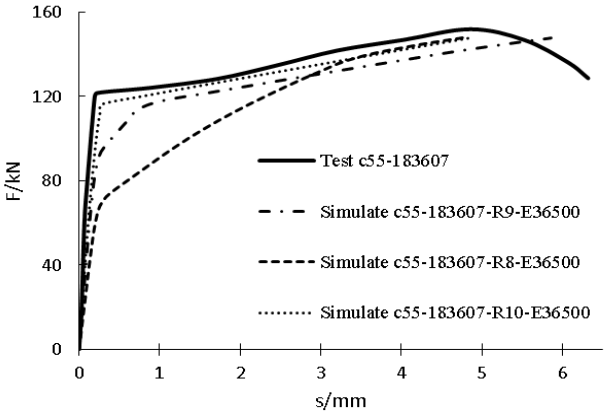

3.3 The practical demonstration

3.3.1 The design and loading test of specimens

The design of specimens

The section size of constrained slurry anchor steel bar connection specimen is 150 mm × 150 mm, and the strength of concrete is C30 and adopt HRB400 lap bars which diameter is 12 mm, also employ HPB235 spiral stirrups which the diameter is 4 mm. Change lap lengths and the ductility of spiral stirrups that is controlled by the spiral hoop diameter D and the stirrup spacing *S*. Figure 7 shows the structure of specimens and parameters are shown in Table 3.

Table 3 The parameters of specimen

Lap bar diameter (mm)	*Lap length(mm)*	*spiral hoop diameter D(mm)*	*Stirrup type*
12	210	60	ϕ4@40

The loading test of specimens

The experiment method has been changed which refer to the General Technical Specification for Steel Bar Mechanical Connection (JGJ107) on the literature (Ni, 2006), and the method of loading tests as follows: ① $0 \to 0.6 f_{yk}$ $(\text{repeat5 times}) \to$ Failure occurs，② $0 \to 0.9 f_{yk}$ $(\text{repeat20 times}) \to$ Failure occurs. The specimen is fixed at one end and the load test is applied to the other end. Figure 8 shows the loading test of specimens.

Figure 7 The structure of specimens

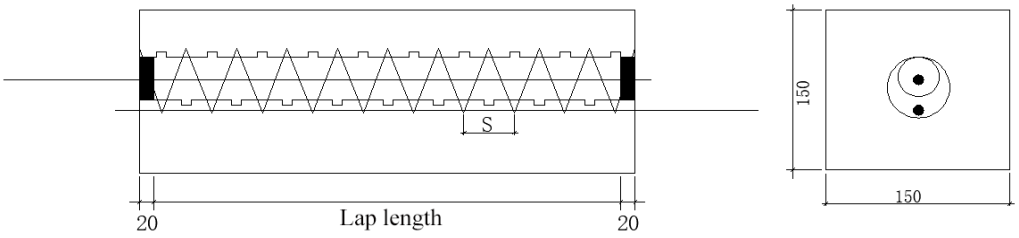

Figure 8 The loading test of specimens.

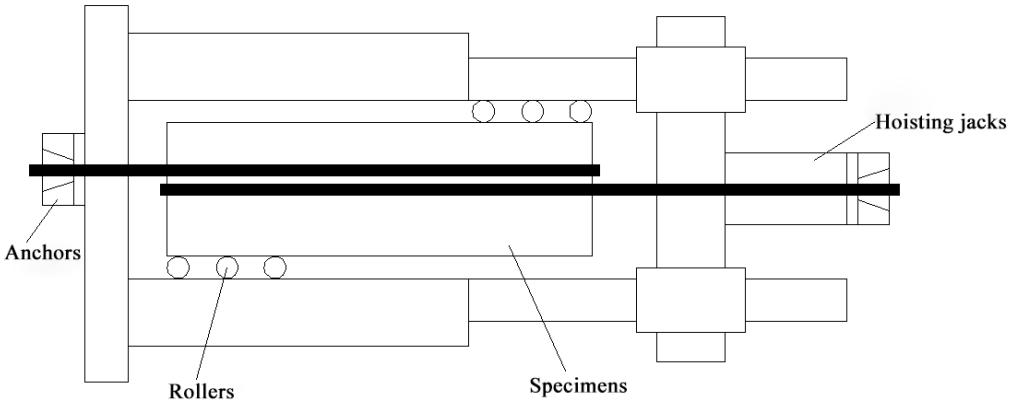

3.3.2 The materials of specimens

The unrevealed mechanical parameters of lap bars are measured through experiments, and HPB235 steel bars was adopted in the test of lap stirrup in the literature (Ni, 2006). The study used strength parameters of HPB235 steel bars from the literature (Lu, 2023). Table 4 shows material parameters of steel bars in the finite element calculation.

Table 4 Reinforcement material parameter

Bar diameter (mm)	*Density (T/mm^3)*	*Es (MPa)*	*Poisson's ratio*	σ_s *(MPa)*	σ_u *(MPa)*	ε_u
12	7.85×10^{-9}	201000	0.3	424.6	620.4	0.205

C30 strength concrete was used and compressive strength data of concrete were measured by experiments in the literature (Ni, 2006). The concrete material and plastic-damage parameters in the finite element calculation on this study are shown in Table 5.

The specimens used YHSCG special cement grouting materials. The strength of grouting material was measured by experiments in the literature (Ni, 2006). The material parameters of beam element in finite element calculation are shown in Table 6. E_1 is the elastic modulus of grout and σ_1 is the compressive strength of grout.

3.3.3 Results and analysis

This study adopted 'spring-beam element' model to test specimens 12-4@40-1and 12-4@40-2 from the literature (Ni, 2006) by trial and error, and adjusted appropriate section parameters of the beam element. Table 7 shows simulation results of the test.

By comparing the simulation results and experiment results of the specimen 12-4@40 under two different conditions, firstly, constitutive model parameters for calculating the fracture of the beam element can be uniquely determined, and the radius (R=5.4 mm) of the beam element section under different loading methods also can be identified, which ensure that simulation results (bearing capacity, residual deformation and slippage) are most close to experiment results. Secondly, it is found that set E_1 as the grouting materials elastic modulus and σ_1 as the compressive strength, which are optimal in the beam element fracture constitutive model calculation, and other parameters need to be calculated. Besides, the theory and practice proved that the fracture constitutive calculation model of the beam element and the radius of the beam element section can be accurately determined with different reinforcements through hosts of experiment and simulation comparisons, which can replace the experiments of anchor lapping structure system under various working conditions.

Table 5 Concrete material and plastic damage parameters

Density (T/mm^3)	E_0 *(MPa)*	*Poisson's ratio*	*Expansion Angle*	F_{b0}/f_{c0}	*Eccentricity*	*K*	*Viscosity parameter*
2.50×10^{-9}	30000	0.2	40	1.16	0.1	0.67	0.05

Table 6 Beam element material parameters

E_1*(MPa)*	σ_1*(MPa)*	σ_2*(MPa)*	ε_e	ε_p	ε_b
36500	73.43	5	0.011	0.03	0.031

Table 7 Simulation and experiment results of specimens 12-4@40-1and 12-4@40-2

Specimen number	*Acquisition method*	*R (mm)*	*Displacement(mm)*	*Bearing capacity (kN)*	*Residual deformation (mm)*	*Slippage(mm)*
12-4@40-1	Simulation	5.3	0.3993	57.67	0.0178	0.2177
		5.4	0.3669	59.12	0.0293	0.1986
		5.5	0.3763	57.27	0.0222	0.2276
		5.6	0.3591	57.79	0.0329	0.1988
		5.7	0.3350	58.03	0.0314	0.1850
	Experiment			62.00	0	0.1500
12-4@40-2	Simulation	5.3	0.376	60.16	0.0699	0.1040
		5.4	0.364	59.65	0.0398	0.0912
		5.5	0.357	57.55	0.0781	0.0958
		5.6	0.345	57.29	0.0855	0.0805
		5.7	0.332	61.54	0.0541	0.0734
	Experiment			70	0	0.04

4 Conclusions

1 E_2 is the condition of the mortar fracture constitutive model controlling the generation of slip damage;

2 There must exist a unique ε_p for the mortar fracture constitutive model to establish;

3 E_1 reflects how close the simulated force-deformation curve is to the one obtained from the test;

4 Theoretically there exists such an elastic modulus making the simulated force-deformation curve coincide with the one obtained from tests;

5 Hosts of tests are conducted to align with the simulation results, and a sufficient number of E_1, ε_p and R_{beam} values under different boundary conditions are obtained, and an ideal model for predicting the E_1, ε_p and R_{beam} values is trained by establishing a neural network model.

Acknowledgement

This paper is financially supported by the Scientific Research Project of Education Department of Jilin Province (Grant No. JJKH20221213KJ) in the design of the study and collection of data.

References

Guo, J., Hu, S. and Qi, H. et al. (2022) 'Experimental study on anchorage property of rebar-metallic bellows slurry anchor connection considering grout age', *Journal of Civil and Environmental Engineering*, pp.1–10. Available online at: http://kns-cnki-net.webvpn.ccit.edu.cn/kcms/detail/50.1218.tu.20220624.1705.002.html

He, Y. (2020) 'Experimental study on pull-out capacity of rebar anchored in embedded corrugated sleeve in the concrete-filled steel tubular', *Chang sha: Hunan University*, pp.14–42.

Hosseini, S.J.A. and Rahman, A.B.A. (2016) 'Effects of spiral confinement to the bond behavior of deformed reinforcement bars subjected to axial tension', *Engineering Structure*, Vol. 112, pp.1–13.

Hosseini, S.J.A., Rahman, A.B.A. and Osman, M.H. et al. (2015) 'Bond behavior of spirally confined splice of deformed bars in grout', *Construction and Building Materials*, Vol. 80, pp.180–194.

Lu, H. (2023) 'Study on shear performance of assembled reinforced concrete beams with steel joints', *Building Structure,* Vol. 53, No. 9, pp.115–122.

Ni, Y. (2006) 'Experimental research on the ultimate lap length of the restraint grouting anchoring overlap joint of steel bar', *Harbin: Harbin Institute of Technology*, pp.1–89.

Nie, H., Yu, Y. and Li, L. (2022) 'Put forward spring-beam-block element model for the finite element calculation of grouting sleeve connection', *Science Technology and Industry*, Vol. 22, No. 3, pp.297–303.

Shi, P., Wang, H. and Liu, J. et al. (2021) 'Numerical analysis of anchorage properties of grouting connection of pre-buried bellows with steel bars inserted', *Journal of Harbin Engineering University*, Vol. 42, No. 6, pp.810–817.

Wu, D., Liang, S. and Guo, Z. et al. (2020) 'Experiment study on spatial structural model with grouted connected precast shear-wall,' *Journal of Building Structure*, Vol. 41, No. 7, pp.110–116.

Wu, Y., Xiao, Y. and Anderson, J.C. (2009) 'Seismic behavior of PC column and steel beam composite moment frame with posttensioned connection', *Journal of structural engineering*, Vol. 135, No. 11, pp.1398–1407.

Xie, K., Gu, Q. and Wang, Z. (2018) 'Study on precast PC components connection of steel joint performance', *Concrete*, Vol. 2, pp.124–129.

Zhao, J., Zhou, L. and Ding, Y. et al. (2023) 'Experiment on anchoring performance of spiral stirrup-corrugated pipe grout splicing', *Journal of Jilin University (Engineering and Technology Edition)*. Available online at: https://kns.cnki.net/kcms/detail/22.1341.T.20230327.0904.004.html

Zhou, W., Wu, M. and Li, S. et al. (2021a) 'Study on spring-rod element model for the finite element calculation of prefabricated slurry anchor connection', *Journal of Shenyang Ligong University*, Vol. 40, No. 5, pp.72–78.

Zhou, W., Yu, Y. and Wu, M. et al. (2021b) 'A spring-beam element model for the finite element calculation of prefabricated slurry anchor connection', *Journal of Water Resources and Architectural Engineering*, Vol. 19, No. 4, pp.144–149.